

Effect of weak impurities on electronic properties of graphene: functional renormalization-group analysis

A. Katanin

*Institute of Metal Physics, 620990, Ekaterinburg, Russia,
and Ural Federal University, 620002, Ekaterinburg, Russia*

We consider an effect of weak impurities on electronic properties of graphene within the functional renormalization-group approach. The energy dependences of the electronic self-energy and density of states near the neutrality point are discussed. Depending on the symmetry of the impurities, the electronic damping Γ and density of states ρ can deviate substantially from those given by the self-consistent Born approximation. We investigate the crossover from the results of the self-consistent Born approximation, which are valid far from the neutrality point to the strong-coupling (diffusive) regime near the neutrality point. For impurities, which are diagonal in both, valley and sublattice indices, we obtain finite density of states at the Fermi level with the values, which are much bigger than the result of self-consistent Born approximation.

Graphene is a two-dimensional system with the Dirac electronic dispersion, that possesses unique properties. In particular, the electronic properties of graphene near the neutrality point remain a challenging problem of condensed-matter physics. Unlike many two-dimensional systems, the conductivity remains finite at the neutrality point[1]. Although the density of states (DOS) for systems with Dirac dispersion is expected to vanish at the neutrality point, finite DOS at the corresponding position of the Fermi level was observed experimentally in graphene[2].

The electronic properties of graphene are expected to be strongly influenced by impurities. Although the chiral disorder does not lead to the localization[3, 4], this particular type of disorder is realized only for infinitely strong impurities (e.g. vacancies). The effect of strong impurities was intensively investigated within both, analytical [5] and numerically exact approaches[6, 7].

At the same time, even weak impurities may have non-trivial effect on the electronic properties of graphene. In particular, the chiral disorder of the CI symmetry class was argued to yield the energy dependence $\epsilon^{1/7}$ of the density of states near the neutrality point[8]. This result is distinctly different from that of the self-consistent Born approximation (SCBA) [9], considering only multiple scattering of electrons on the same impurity, which enlightens the importance of inter-impurity scattering processes. It was also shown in Ref. [4] that for the long-range disorder, which is diagonal in both valley and sublattice spaces, SCBA predicts much smaller damping of electrons close to the neutrality point, than expected from other approaches.

The standard renormalization-group (RG) approach of Ref. [4] allows to describe inter-impurity scattering, but it treats the ballistic regime of the flow only. In particular, this approach yields divergence of the vertices at some critical length scale, which does not allow to describe the crossover to the strong-coupling (diffusive) regime. Investigation of the diffusive regime represents, however, an important problem, since it allows to describe physical properties in the range of fillings close to

the neutrality point. Although some results for the density of states and conductivity were obtained within the nonlinear-sigma model approach (see, e.g., Refs. [4, 8, 10] and references therein), it is interesting to perform the analysis starting from the weak-coupling point of view, which may allow to treat both the strong-coupling (diffusive) regime of the flow and the crossover from ballistic to diffusive regime.

In this paper we investigate the effect of long-range and chiral potential impurities on the electronic properties of graphene within the recently proposed Wick-ordered functional renormalization group scheme[12, 13], allowing to treat self-energy effects beyond the leading order of perturbation theory.

We consider quartic interaction between Dirac fermions due to averaged potential impurity scattering. Assuming only second-order cumulants are important (i.e. the impurity potentials are substantially weak) the corresponding action reads[4, 14]

$$S = \int d^2x \left[\int d\tau \bar{\psi}(\gamma_\mu \partial_\mu) \psi - \frac{1}{2} n_{\text{imp}} \sum_l T_l^2 \int d\tau \int d\tau' (\bar{\psi}_\tau M_l \psi_\tau) (\bar{\psi}_{\tau'} M_l \psi_{\tau'}) \right] \quad (1)$$

where $\mu = 0, 1, 2$, $\partial = (\partial_\tau, v_F \partial_x, v_F \partial_y)$, $\bar{\psi} = \psi^\dagger \gamma_0$, γ_μ are the Dirac matrices, e.g.

$$\gamma_0 = \begin{pmatrix} \sigma_3 & 0 \\ 0 & -\sigma_3 \end{pmatrix}, \quad \gamma_a = \begin{pmatrix} \sigma_a & 0 \\ 0 & -\sigma_a \end{pmatrix}, \quad (2)$$

where $a = 1, 2$, σ_i are the Pauli matrices. The quadratic part of the action (1) represents the continuum limit of the microscopic tight-binding model (see, e.g., Refs. [4, 14]) and corresponds to the representation $\psi = \{\psi_A^1, \psi_B^1, \psi_B^2, -\psi_A^2\}$ (ψ_s^m is an annihilation operator for the electron in valley m and sublattice s). The quantities T_l represent scattering amplitudes (impurity potentials) in different channels; the latter are described by 4×4 matrices M_l , belonging to a linearly independent set of complex matrices with $(\gamma_0 M_l)^2 = I$ (I - identity

matrix). The interaction in Eq. (1) is obtained after averaging over impurity positions with $\langle U_l(\mathbf{x})U_l(\mathbf{x}') \rangle = n_{\text{imp}} T_l^2 \delta^{(2)}(\mathbf{x} - \mathbf{x}')$, n_{imp} is the impurity concentration. Eq. (1) neglects higher than second order scattering processes on the same impurity, which implies that this equation is applicable in the limit of weak impurities, $2\pi n_{\text{imp}} [T_l/(2\pi v_F)]^n \ll 1$ for $n \geq 1$.

The mean-field (self-consistent Born) approximation for the model (1) yields for the fermionic self-energy $\hat{\Sigma}^\varepsilon$ (see, e.g. Ref. [4] and references therein)

$$\hat{\Sigma}^\varepsilon = -n_{\text{imp}} \sum_{\mathbf{k}, l} T_l^2 M_l \frac{1}{\gamma_0 \varepsilon - \hat{\Sigma}^\varepsilon + i v_F \gamma_a k_a} M_l \quad (3)$$

Taking into account that $(M_l \gamma_0)^2 = I$, the solution to this equation has the form $\hat{\Sigma}^\varepsilon = \gamma_0 \Sigma(\varepsilon)$ with

$$\Sigma(\varepsilon) = \frac{U^2 n_{\text{imp}}}{4\pi v_F^2} [\varepsilon - \Sigma(\varepsilon)] \ln \frac{-(v_F \Lambda_{\text{uv}})^2}{[\varepsilon - \Sigma(\varepsilon)]^2} \quad (4)$$

where $U^2 = \sum_l T_l^2$, and Λ_{uv} is an ultraviolet momentum cutoff. At $\varepsilon \rightarrow 0$ equation (4) yields [4]

$$\Sigma(0) = -i\Gamma; \quad \Gamma \simeq \Lambda_{\text{uv}} e^{-2\pi v_F^2/(n_{\text{imp}} U^2)} \quad (5)$$

Note that exponential smallness of Γ in graphene in the limit of weak impurities is due to vanishing of the density of states of pure system at the Fermi level. The density of states of impure system at the Fermi level in SCBA reads [4]

$$\rho(0) = \frac{4\Gamma}{\pi n_{\text{imp}} U^2} \quad (6)$$

The renormalization group. To treat the effect of weak impurities beyond SCBA, we apply the recently proposed Wick-ordered functional renormalization-group scheme [11–13] by considering the sharp momentum cut-off of the electronic propagator in the form

$$C_\Lambda = \left(\gamma_0 \varepsilon - \hat{\Sigma}_\Lambda^\varepsilon + i v_F \gamma_a k_a \right)^{-1} \theta(|\mathbf{k}| - \Lambda) \quad (7)$$

where Λ is the cutoff parameter. The corresponding single-scale propagator reads

$$S_\Lambda = -\dot{C}_\Lambda + C_\Lambda \hat{\Sigma}_\Lambda^\varepsilon C_\Lambda = \left(\gamma_0 \varepsilon - \hat{\Sigma}_\Lambda^\varepsilon + i v_F \gamma_a k_a \right)^{-1} \delta(|\mathbf{k}| - \Lambda), \quad (8)$$

the dot stands for the derivative over Λ . Following Refs. [12, 13], we choose the Wick-ordering propagator in the form, which is complementary to C_Λ :

$$D_\Lambda = \left(\gamma_0 \varepsilon - \hat{\Sigma}_\Lambda^\varepsilon + i v_F \gamma_a k_a \right)^{-1} \theta(\Lambda - |\mathbf{k}|). \quad (9)$$

In the renormalization-group approach we have contribution of three different channels to the vertex renormalization. The replica trick requires that the diagrams with closed loops (i.e., those containing summations over

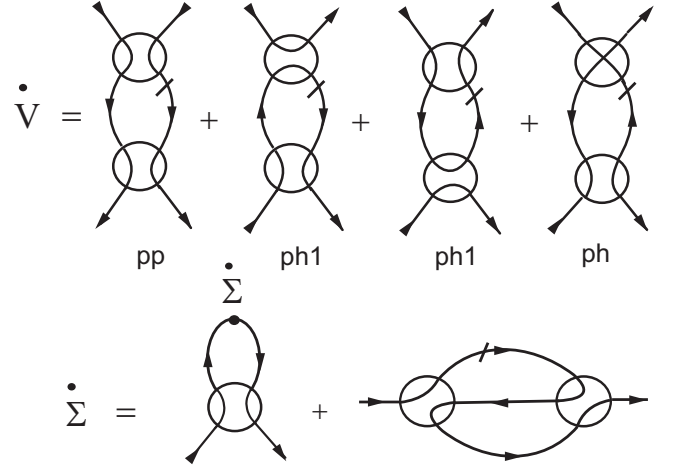


FIG. 1: The diagrammatic form of the RG equations for the interaction vertices and self-energy. Solid lines with dash correspond to the single-scale propagator, Eq. (8), other solid lines connecting vertices – to the Wick propagator (9). Lines inside vertices connect the legs with the same replica index.

number of fermion species) should be excluded from the diagram technique. The corresponding RG equations for the vertex $V_{i_{1..4}}^{\varepsilon\varepsilon'}(\mathbf{k}_1, \mathbf{k}_2, \mathbf{k}_3)$ and the self-energy $\hat{\Sigma}_{i_{1..4}}^\varepsilon(i_{1,2}, \mathbf{k}_{1,2}$ and $i_{3,4}, \mathbf{k}_{3,4}$ correspond to valley-sublattice indices and momenta of incoming and outgoing particles, ε and ε' are the energies of the interacting particles) are presented in the Supplementary material and shown diagrammatically in Fig. 1.

To solve the RG equations numerically we decompose the vertex into the contribution of particle-hole direct and crossed (ph and ph1), and particle-particle (pp) channels similarly to Ref. [15],

$$V_{i_{1..4}}^{\varepsilon\varepsilon'}(\mathbf{k}_1, \mathbf{k}_2, \mathbf{k}_3) = V_{i_{1..4}}^{\varepsilon\varepsilon', \text{ph}}(\mathbf{k}_3 - \mathbf{k}_2) + V_{i_{1..4}}^{\varepsilon\varepsilon', \text{ph1}}(\mathbf{k}_1 - \mathbf{k}_3) + V_{i_{1..4}}^{\varepsilon\varepsilon', \text{pp}}(\mathbf{k}_1 + \mathbf{k}_2). \quad (10)$$

Assuming that the disorder is time-reversal invariant, we also use symmetries of the interaction $V_{i_{1..4}}^{\varepsilon\varepsilon', \text{ph}}(\mathbf{q}) = T_{i_2 i_2'} V_{i_1 i_2' i_3 i_4'}^{\varepsilon\varepsilon', \text{pp}}(\mathbf{q}) T_{i_4' i_4}$, $V_{i_{1..4}}^{\varepsilon\varepsilon', \text{ph1}}(\mathbf{q}) = T_{i_2 i_2'} V_{i_1 i_2' i_3 i_4'}^{\varepsilon\varepsilon', \text{ph1}}(\mathbf{q}) T_{i_4' i_4}$ where $T = i\gamma_1 \gamma_3$ is the time-inversion matrix, $\gamma_3 = \begin{pmatrix} 0 & iI \\ -iI & 0 \end{pmatrix}$ and put $\varepsilon' = \varepsilon$, since we consider only retarded channel of electronic scattering. The initial conditions for the RG equations read $V_{i_{1..4}}^{\varepsilon\varepsilon} |_{\Lambda=\Lambda_{\text{uv}}} = n_{\text{imp}} \sum_l T_l^2 M_l^{i_1 i_3} M_l^{i_2 i_4}$; $\hat{\Sigma}_{\Lambda=\Lambda_{\text{uv}}}^\varepsilon = -i\Gamma \gamma_0$.

Results. Below we consider the long-range disorder, diagonal in both sublattice and valley subspaces ($2 \times \text{AII}$ symmetry class), which corresponds to $M_1 = \gamma_0$, $T_l = U \delta_{l,1}$, and one of the chiral disorders preserving time-reversal symmetry $T M_l^T T = M_l$ with matrices $M_l \in \{i\gamma_{1,2}\gamma_3, i\gamma_{1,2}\gamma_5\}$ describing intervalley scattering of fermions in each of the sublattices ($\gamma_5 = -\gamma_0 \gamma_1 \gamma_2 \gamma_3$), $T_l = U/2$. Although realistic impurities yield in fact both these types of disorder (see, e. g., Ref. [4]), for

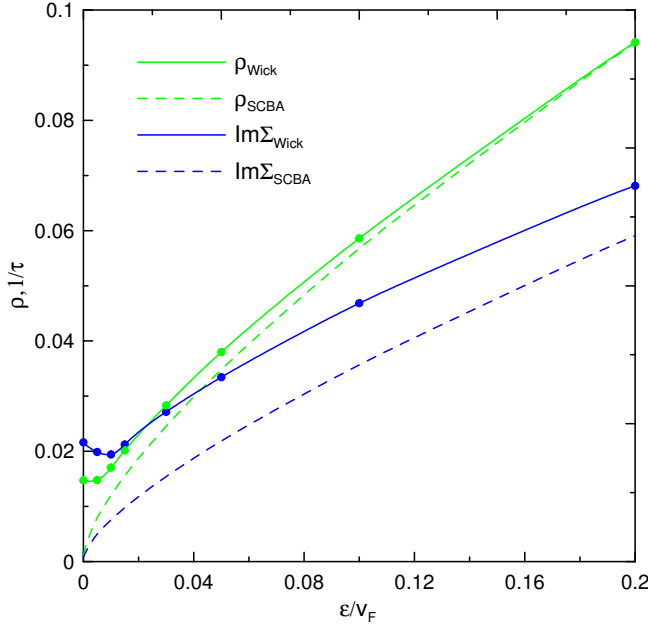


FIG. 2: (Color online) The imaginary part of the self-energy and the density of states (in units of v_F) at different energy distance to the neutrality point for long-range diagonal disorder.

theoretical analysis it is informative to consider these types separately. The flow for these types of the disorder at the scales $\Lambda \gg |\text{Im}\Sigma|/v_F$, i.e. in the ballistic regime, when one can neglect the quasiparticle damping, was discussed in detail in Ref. [4] (see also references therein). In particular, both disorders, γ_0 and $i\gamma_{1,2\gamma_{3,5}}$ yield the flow of the coupling constants to the strong-coupling regime. For our numerical calculations we use the parameters $U^2 n_{\text{imp}}/v_F^2 = 0.8$, $\Lambda_{\text{uv}} = 2$. The corresponding SCBA damping is $\Gamma = 7.76 \cdot 10^{-4} v_F$. The results of our fRG analysis are presented in Figs. 2-5.

For γ_0 (long-range diagonal) disorder we find saturation of the density of states and imaginary part of the self-energy at values, which are much larger than the SCBA results (see Fig. 2). This agrees with earlier observation in Ref. [4], that the critical scale of the divergence of vertices in the standard RG analysis Λ_{min} differs from the SCBA result (5) by a factor of 2 in the exponent (for the considered parameters we find $\Lambda_{\text{min}} \simeq 0.04$). Present analysis yields however finite vertices at and below the critical scale Λ_{min} (Fig. 3). This is due to the cutoff of the divergence of vertices in the present approach by the quasiparticle damping, which occurs since renormalization of the vertices involves dressed rather than bare Green functions and reflects non-perturbative character of the considering approach (cf. the flow into the magnetic, superconducting, or charge-ordered phases within the one-particle functional renormalization group approach [16]). From the field-theoretic point of view, this corresponds to account of many-loop diagrams within the considered truncation of RG hierarchy. Using SCBA

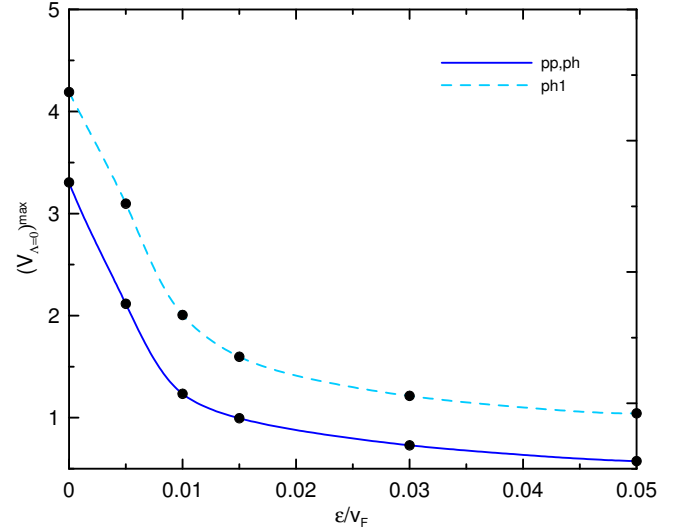


FIG. 3: (Color online) The maximal interaction vertex in the end of the fRG flow as a function of the energy distance to the neutrality point for long-range diagonal disorder.

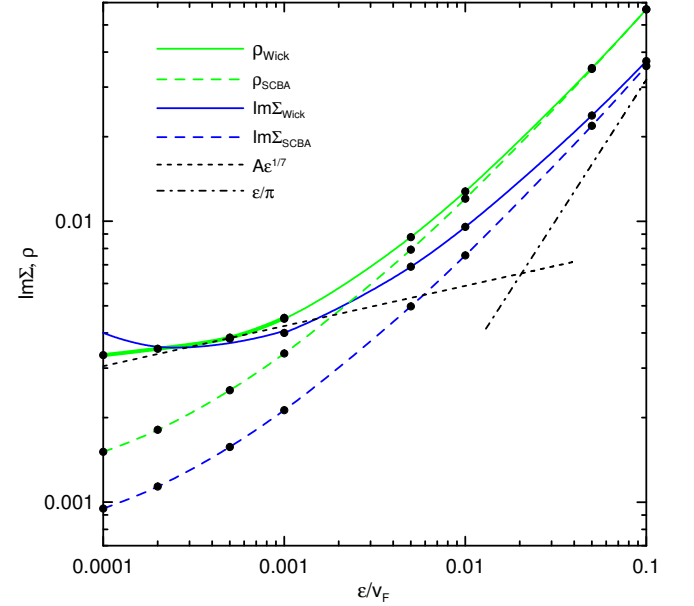


FIG. 4: (Color online) The same as Fig.1 for chiral disorder of CI symmetry class.

self-energy as an input of RG flow in the present approach allows us to treat these self-energy effects more efficiently, since vertices do not grow strongly already from the beginning of the flow. The finiteness of the vertices (which divergences are cut at the quasiparticle damping) allows us to describe the crossover between the ballistic ($|\varepsilon| \gg |\text{Im}\Sigma|$) and the diffusive ($|\varepsilon| \ll |\text{Im}\Sigma|$) regimes at the energy $\varepsilon_{\text{cross}} \simeq 0.02v_F \sim \Lambda_{\text{min}}v_F$ and obtain density of states and quasiparticle life-time near the neutrality point. In particular, the quasiparticle damping approaches the value, which is approximately equal

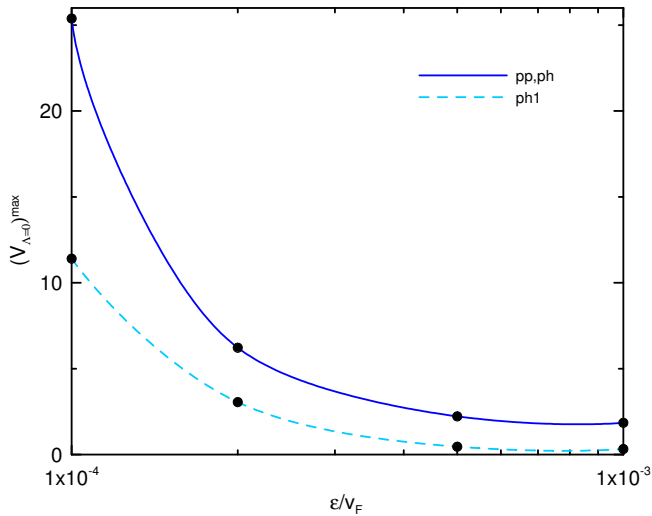


FIG. 5: (Color online) The same as Fig. 2 for chiral disorder of CI symmetry class

to the crossover scale ϵ_{cross} .

For $i\{\gamma_{1,2}\gamma_{3,5}\}$ disorder we find much smaller values of the electronic damping, than for the diagonal disorder (Fig. 4). Moreover, at low energies, logarithm of the density of states scales almost linearly with $\ln \epsilon$, with the slope, which is much smaller, than for SCBA result. The slope of the low-energy region agrees well with that obtained in the strong-coupling analysis of the problem[8], revealing that the density of states is expected to behave as $\rho \sim \epsilon^{1/7}$ at small energies; for the exponent we obtain in the present approach the value 0.1. The values of the maximal vertices, obtained for the considering chiral disorder, are shown in Fig. 5 and grow on approaching neutrality point. This behavior of vertices is similar to that found for certain symmetries of the dis-

order in d -wave superconductors in Ref. [17], and related to approaching chiral symmetry of the considering model at $\epsilon = 0$, which implies poles in the the diffusons and cooperons in retarded-retarded (RR) channel. The obtained momentum dependence of $V^{\epsilon\epsilon, \text{ph}}(\mathbf{k})$ at $\epsilon > 0$ has however a maximum at $k \sim |\text{Im } \Sigma|/v_F$ and approach the corresponding dependence in the retarded-advanced (RA) channel only for very small $\epsilon < 10^{-4}v_F$. As discussed in Ref. [17], the singularity of the RR diffusons provides peculiarities of the density of states, which is likely related to the observed power law behavior of the DOS for CI symmetry.

In Conclusion, we have considered the effect of weak impurities on electronic properties of graphene. For long-range disorder, we find saturation of the density of states at the values, which are much bigger than those obtained previously within the SCBA analysis. On the other hand, for chiral impurities of CI symmetry class we find indications of vanishing density of states at the Fermi level, with the power law, which approximates the previously obtained result $\rho \propto \epsilon^{1/7}$. The functional renormalization-group approach allows to describe the crossover from the ballistic to the diffusive regime in both cases. For realistic impurities, both long-range and chiral components are present. We expect that long-range component will be dominating in this case. The qualitative behavior of density of states in this case agrees with the recent experimental results[2].

Acknowledgements. The author is grateful to I. V. Gornyi and P. Ostrovsky for pointing the attention to the problem of weak impurities in graphene and stimulating discussions on the physics of this material and role of disorder, and to M. Salmhofer for insightful discussions and hospitality at the Institute of Theoretical Physics, Heidelberg, Germany.

-
- [1] K.S. Novoselov, A.K. Geim, S.V. Morozov, D. Jiang, M.I. Katsnelson, I.V. Grigorieva, S.V. Dubonos, A.A. Firsov, *Nature* **438**, 197 (2005).
 - [2] J. Xia, F. Chen, J. Li, and N. Tao, *Nature Nanotech.* **4**, 505 (2009); L. A. Ponomarenko, R. Yang, R. V. Gorbachev, P. Blake, M. I. Katsnelson, K. S. Novoselov, A. K. Geim, *Phys. Rev. Lett.* **105**, 136801 (2010); K. Nagashio, T. Nishimura, and A. Toriumi, ArXiv 1304.3957 (unpublished).
 - [3] R. Gade and F. Wegner, *Nucl. Phys. B* **360**, 213 (1991).
 - [4] P. M. Ostrovsky, I. V. Gornyi, and A. D. Mirlin, *Phys. Rev. B* **74**, 235443 (2006); *Phys. Rev. Lett.* **98**, 256801 (2007); *Eur. Phys. J.: Special Topics* **148**, 63 (2007).
 - [5] M. Titov, P. M. Ostrovsky, I. V. Gornyi, A. Schuessler, A. D. Mirlin, *Phys. Rev. Lett.* **104**, 076802 (2010).
 - [6] T. O. Wehling, S. Yuan, A. I. Lichtenstein, A. K. Geim, M. I. Katsnelson, *Phys. Rev. Lett.* **105**, 056802 (2010); S. Yuan, H. De Raedt, M. I. Katsnelson, *Phys. Rev. B* **82**, 115448 (2010).
 - [7] P. M. Ostrovsky, M. Titov, S. Bera, I. V. Gornyi, A. D. Mirlin, *Phys. Rev. Lett.* **105**, 266803 (2010).
 - [8] A. A. Nersesyan, A. M. Tsvelik, and F. Wenger, *Phys. Rev. Lett.* **72**, 2628 (1994); *Nucl. Phys. B* **438**, 561 (1995).
 - [9] N. M. R. Peres, F. Guinea, A. H. Castro Neto, *Phys. Rev. B* **73**, 125411 (2006)
 - [10] A.W.W. Ludwig, M.P.A. Fisher, R. Shankar, and G. Grinstein, *Phys. Rev. B* **50**, 7526 (1994).
 - [11] M. Salmhofer, *Comm. Math. Phys.* **194**, 249 (1998)
 - [12] M. Salmhofer, *Ann. der Phys.* **16**, 171 (2007).
 - [13] A. Katanin, *J. Phys. A: Math. Theor.* **44**, 495004 (2011).
 - [14] M. S. Foster and I. L. Aleiner, *Phys. Rev. B* **77**, 195413 (2008).
 - [15] C. Husemann and M. Salmhofer, *Phys. Rev. B* **79**, 195125 (2009).
 - [16] W. Metzner, M. Salmhofer, C. Honerkamp, V. Meden, and K. Schoenhammer, *Rev. Mod. Phys.* **84**, 299 (2012).
 - [17] A. G. Yashenkin, W. A. Atkinson, I. V. Gornyi, P. J. Hirschfeld, D. V. Khveshchenko, *Phys. Rev. Lett.* **86**, 5982 (2001).

Supplementary material for the paper "Effect of weak impurities on electronic properties of graphene: functional renormalization-group analysis"

In this material we present analytical form of the renormalization-group equations, shown in Fig. 1 of the paper. The equation for the vertices $V_{i_{1..4}}^{\varepsilon\varepsilon'}(\mathbf{k}_1, \mathbf{k}_2, \mathbf{k}_3)$ reads:

$$\begin{aligned} \dot{V}_{i_{1..4}}^{\varepsilon\varepsilon'}(\mathbf{k}_1, \mathbf{k}_2, \mathbf{k}_3) = & - \sum_{\mathbf{k}, i'_{1..4}} V_{i_1 i'_4 i'_1 i'_4}^{\varepsilon\varepsilon'}(\mathbf{k}_1, \mathbf{k} + \mathbf{k}_2 - \mathbf{k}_3, \mathbf{k}) V_{i'_3 i'_2 i'_3 i'_2}^{\varepsilon\varepsilon'}(\mathbf{k}, \mathbf{k}_2, \mathbf{k}_3) \\ & \times D_{\mathbf{k}}^{i'_1 i'_3}(\varepsilon) S_{\mathbf{k} + \mathbf{k}_3 - \mathbf{k}_2}^{i'_2 i'_4}(\varepsilon') - \\ & \sum_{\mathbf{k}, i'_{1..4}} \left[V_{i_1 i'_1 i'_3 i'_3}^{\varepsilon\varepsilon'}(\mathbf{k}_1, \mathbf{k} + \mathbf{k}_3 - \mathbf{k}_1, \mathbf{k}) V_{i'_4 i'_2 i'_2 i'_4}^{\varepsilon\varepsilon'}(\mathbf{k}, \mathbf{k}_2, \mathbf{k} + \mathbf{k}_3 - \mathbf{k}_1) \right. \\ & \left. + V_{i_1 i'_1 i'_3 i'_3}^{\varepsilon\varepsilon'}(\mathbf{k}_1, \mathbf{k} + \mathbf{k}_3 - \mathbf{k}_1, \mathbf{k}_3) V_{i'_4 i'_2 i'_4 i'_2}^{\varepsilon\varepsilon'}(\mathbf{k}, \mathbf{k}_2, \mathbf{k}_1 + \mathbf{k}_2 - \mathbf{k}_3) \right] \\ & \times D_{\mathbf{k}}^{i'_3 i'_4}(\varepsilon) S_{\mathbf{k} + \mathbf{k}_1 - \mathbf{k}_3}^{i'_2 i'_1}(\varepsilon) \\ & - \sum_{\mathbf{k}, i'_{1..4}} V_{i_1 i'_2 i'_1 i'_2}^{\varepsilon\varepsilon'}(\mathbf{k}_1, \mathbf{k}_2, \mathbf{k}) V_{i'_3 i'_4 i'_3 i'_4}^{\varepsilon\varepsilon'}(\mathbf{k}, -\mathbf{k} + \mathbf{k}_1 + \mathbf{k}_2, \mathbf{k}_3) \\ & \times D_{\mathbf{k}}^{i'_1 i'_3}(\varepsilon) S_{-\mathbf{k} + \mathbf{k}_1 + \mathbf{k}_2}^{i'_2 i'_4}(\varepsilon') + S \rightleftharpoons D. \end{aligned} \quad (11)$$

where the propagators S and D are defined by the Eqs. (8) and (9) of the main text. For the self-energy correction we obtain the equation

$$\begin{aligned} \hat{\Sigma}_{i_1 i_3 \Lambda}^{\varepsilon}(\mathbf{k}) = & \sum_{\mathbf{p}, i'_{1..4}} V_{i_1 i'_2 i'_1 i'_3}^{\varepsilon\varepsilon}(\mathbf{k}, \mathbf{p}, \mathbf{k}) D_{\Lambda}^{i'_1 i'_3}(\mathbf{p}) \hat{\Sigma}_{i'_3 i'_4 \Lambda}^{\varepsilon}(\mathbf{p}) D_{\Lambda}^{i'_4 i'_2}(\mathbf{p}) \\ & - \sum_{\mathbf{p}, i'_{1..6}} V_{i_1 i'_4 i'_1 i'_5}^{\varepsilon\varepsilon}(\mathbf{k}, \mathbf{q}, \mathbf{p}) V_{i'_2 i'_6 i'_5 i'_3}^{\varepsilon\varepsilon}(\mathbf{p}, \mathbf{k} + \mathbf{q} - \mathbf{p}, \mathbf{q}) \\ & \times S_{\Lambda}^{i'_1 i'_2}(\mathbf{p}) D_{\Lambda}^{i'_3 i'_4}(\mathbf{q}) D_{\Lambda}^{i'_5 i'_6}(\mathbf{k} + \mathbf{q} - \mathbf{p}) \\ & + 2 \text{ perm. } S \rightleftharpoons D]. \end{aligned} \quad (12)$$

Using the ansatz (10) we split contribution from the particle-hole and particle particle channels to the vertex evolution. To obtain contribution of the direct particle-hole channel, we put in Eq. (11) $\mathbf{k}_1 = -\mathbf{k}_2 = \mathbf{k}_3 = \mathbf{q}/2$, and obtain

$$\begin{aligned} \dot{V}_{i_{1..4}}^{\varepsilon\varepsilon', \text{ph}}(\mathbf{q}) = & \sum_{i'_{1..4}, \mathbf{k}} \left[V_{i_1 i'_4 i'_1 i'_4}^{\varepsilon\varepsilon', \text{ph}}(\mathbf{q}) + V_{i_1 i'_4 i'_1 i'_4}^{\varepsilon\varepsilon', \text{ph1}}\left(\frac{\mathbf{q}}{2} - \mathbf{k}\right) + V_{i_1 i'_4 i'_1 i'_4}^{\varepsilon\varepsilon', \text{pp}}\left(\mathbf{k} - \frac{\mathbf{q}}{2}\right) \right] \\ & \times \left[V_{i'_3 i'_2 i'_3 i'_2}^{\varepsilon\varepsilon', \text{ph}}(\mathbf{q}) + V_{i'_3 i'_2 i'_3 i'_2}^{\varepsilon\varepsilon', \text{ph1}}\left(\mathbf{k} - \frac{\mathbf{q}}{2}\right) + V_{i'_3 i'_2 i'_3 i'_2}^{\varepsilon\varepsilon', \text{pp}}\left(\mathbf{k} - \frac{\mathbf{q}}{2}\right) \right] \\ & \times \{ S_{\mathbf{k}}^{i'_1 i'_3}(\varepsilon) D_{\mathbf{k} - \mathbf{q}}^{i'_2 i'_4}(\varepsilon) + S \rightleftharpoons D \}; \end{aligned} \quad (13)$$

Putting in Eq. (11) $\mathbf{k}_1 = -\mathbf{k}_2 = -\mathbf{k}_3 = \mathbf{q}/2$, we obtain

$$\begin{aligned} \dot{V}_{i_{1..4}}^{\varepsilon\varepsilon', \text{ph1}}(\mathbf{q}) = & \sum_{i'_{1..4}, \mathbf{k}} \left\{ \left[V_{i_1 i'_1 i'_3 i'_3}^{\varepsilon\varepsilon', \text{ph}}(\mathbf{q}) + V_{i_1 i'_1 i'_3 i'_3}^{\varepsilon\varepsilon', \text{ph1}}\left(\frac{\mathbf{q}}{2} - \mathbf{k}\right) + V_{i_1 i'_1 i'_3 i'_3}^{\varepsilon\varepsilon', \text{pp}}\left(\mathbf{k} - \frac{\mathbf{q}}{2}\right) \right] \right. \\ & \times \left[V_{i'_4 i'_2 i'_2 i'_4}^{\varepsilon\varepsilon', \text{ph}}\left(\mathbf{k} - \frac{\mathbf{q}}{2}\right) + V_{i'_4 i'_2 i'_2 i'_4}^{\varepsilon\varepsilon', \text{ph1}}(\mathbf{q}) + V_{i'_4 i'_2 i'_2 i'_4}^{\varepsilon\varepsilon', \text{pp}}\left(\mathbf{k} - \frac{\mathbf{q}}{2}\right) \right] \\ & + \left[V_{i_1 i'_1 i'_3 i'_3}^{\varepsilon\varepsilon', \text{ph}}\left(\frac{\mathbf{q}}{2} - \mathbf{k}\right) + V_{i_1 i'_1 i'_3 i'_3}^{\varepsilon\varepsilon', \text{ph1}}(\mathbf{q}) + V_{i_1 i'_1 i'_3 i'_3}^{\varepsilon\varepsilon', \text{pp}}\left(\mathbf{k} - \frac{\mathbf{q}}{2}\right) \right] \\ & \times \left[V_{i'_4 i'_2 i'_4 i'_2}^{\varepsilon\varepsilon', \text{ph}}(\mathbf{q}) + V_{i'_4 i'_2 i'_4 i'_2}^{\varepsilon\varepsilon', \text{ph1}}\left(\mathbf{k} - \frac{\mathbf{q}}{2}\right) + V_{i'_4 i'_2 i'_4 i'_2}^{\varepsilon\varepsilon', \text{pp}}\left(\mathbf{k} - \frac{\mathbf{q}}{2}\right) \right] \left. \right\} \\ & \times \{ S_{\mathbf{k}}^{i'_3 i'_4}(\varepsilon) D_{\mathbf{k} - \mathbf{q}}^{i'_2 i'_1}(\varepsilon) + S \rightleftharpoons D \}; \end{aligned} \quad (14)$$

Finally, putting in Eq. (11) $\mathbf{k}_1 = \mathbf{k}_2 = \mathbf{k}_3 = \mathbf{q}/2$, we obtain

$$\begin{aligned} \dot{V}_{i_{1..4}}^{\varepsilon\varepsilon', \text{pp}}(\mathbf{q}) = & \sum_{i'_{1..4}, \mathbf{k}} \left[V_{i_1 i'_2 i'_1 i'_2}^{\varepsilon\varepsilon', \text{ph}}\left(\mathbf{k} - \frac{\mathbf{q}}{2}\right) + V_{i_1 i'_2 i'_1 i'_2}^{\varepsilon\varepsilon', \text{ph1}}\left(\frac{\mathbf{q}}{2} - \mathbf{k}\right) + V_{i_1 i'_2 i'_1 i'_2}^{\varepsilon\varepsilon', \text{pp}}(\mathbf{q}) \right] \\ & \times \left[V_{i'_3 i'_4 i'_3 i'_4}^{\varepsilon\varepsilon', \text{ph}}\left(\mathbf{k} - \frac{\mathbf{q}}{2}\right) + V_{i'_3 i'_4 i'_3 i'_4}^{\varepsilon\varepsilon', \text{ph1}}\left(\mathbf{k} - \frac{\mathbf{q}}{2}\right) + V_{i'_3 i'_4 i'_3 i'_4}^{\varepsilon\varepsilon', \text{pp}}(\mathbf{q}) \right] \\ & \times \{ S_{\mathbf{k}}^{i'_1 i'_3}(\varepsilon) D_{-\mathbf{k} + \mathbf{q}}^{i'_2 i'_4}(\varepsilon') + S \rightleftharpoons D \} \end{aligned} \quad (15)$$

The number of vertices per every set $\varepsilon, \varepsilon'$ is $3 \cdot 256 \cdot n_k$ where n_k is the number of the considered k -points. The equations (12)-(15) have to be solved numerically. For the numerical solution, we expand vertices $V_{i_{1..4}}^{\varepsilon\varepsilon', c}(\mathbf{q})$ ($c = \text{ph}, \text{ph1}, \text{or pp}$) in each of the channels in harmonics

$$\begin{aligned} V_{i_{1..4}}^{\varepsilon\varepsilon', c}(\mathbf{q}) = & \sum_{m=0}^n \left[F_{i_{1..4}}^{\varepsilon\varepsilon', cm}(q) \cos(m\varphi_{\mathbf{q}}) \right. \\ & \left. + G_{i_{1..4}}^{\varepsilon\varepsilon', cm}(q) \sin(m\varphi_{\mathbf{q}}) \right] \end{aligned} \quad (16)$$

where $\varphi_{\mathbf{q}}$ is the polar angle of the vector \mathbf{q} . In the numerical solution we take 12 points in radial q direction and account for $n + 1 = 3$ harmonics in Eq. (16). The results of the solution of Eqs. (13)-(16) are discussed in the main text.